NASA Technical Memorandum 101530

FLUTTER ANALYSIS OF HIGHLY SWEPT DELTA WINGS BY CONVENTIONAL METHODS

M. D. GIBBONS
D. L. SOISTMANN
R. M. BENNETT

NOVEMBER 1988

National Aeronautics and
Space Administration

Langley Research Center
Hampton, Virginia 23665-5225

FLUTTER ANALYSIS OF HIGHLY SWEPT DELTA WINGS BY CONVENTIONAL METHODS

M. D. Gibbons
D. L. Soistmann
PRC Systems Services
Hampton, Virginia 23666

R. M. Bennett
NASA Langley Research Center
Hampton, Virginia 23665-5225

Abstract

The flutter boundaries of six thin highly-swept delta-planform wings have been calculated. Comparisons are made between experimental data and results using several aerodynamic methods. The aerodynamic methods used include a subsonic and supersonic kernel function, second order piston theory, and a transonic small disturbance code. The dynamic equations of motion are solved using analytically calculated mode shapes and frequencies.

Nomenclature

A	aspect ratio
b	root semichord
M_∞	freestream Mach number
t	thickness of wing
V_f	flutter speed
W	total weight of wing
δ	length of bevel
μ	mass density parameter
ω_i	natural frequency of i th mode

ω_f flutter frequency

Introduction

The highly-swept delta wings found on typical NASP configurations and the associated flutter boundaries of such wings are of current interest. To study this problem it is helpful to first examine simple configurations for which test data is available such as wing-alone flate-plate models. Confidence can then be built in predicting flutter boundaries of such highly swept delta wings prior to studying more complex configurations. The aerodynamic methods used in calculating the flutter boundaries include FAST, ACUNN, second order piston theory and CAP-TSD. The first three methods were used to calculate the flutter boundaries of six delta wings for which experimental data exists in a report by Hanson and Levey[1]. CAP-TSD was used to calculate the flutter boundary of only one delta wing. The experimental flutter data ranges from about Mach 0.6 to Mach 3.0. All six of the wings have modes that are highly cambered. Three or four measured modes were supplied in reference 1, however analytically calculated mode shapes were used. The purpose of the present paper is to provide an assessment of conventional flutter analysis methods by presenting calculated flutter characteristics for these wings. The related topics of angle-of-attack effects including vortex flows on such wings, and of pivoted controls of similar planforms are not considered.

Description of Models and Test

The six wings of reference 1 included three delta wings having 70°, 75°, and 80° leading edge sweep, and three clipped delta wings having a taper ratio of 2/3, and of leading edge sweep 54°, 62°, and 71°. Planforms of the six delta wings tested by Hanson and Levey[1] are shown in Fig. 1. Each of the models tested was of constant thickness except for leading and trailing edge

bevels. All six models had a root chord of one foot with the clipped-tip delta models having a taper ratio of 2/3. The three delta wings with leading edge sweep of 70°, 75°, and 80° are referred to as Wings 1A, 1B, and 1C, respectively. The three clipped-tip delta wings with leading edge sweeps of 54°, 62°, and 71° are referred to as Wings 2A, 2B, and 2C, respectively.

The above models were mounted as shown in Fig. 2 and were tested in the 9 inch x 18 inch blowdown supersonic aeroelasticity tunnel at the NASA Langley Research Center (which currently no longer exists). The degree of rigidity of their mounting apparently caused some fluctuation in the modal frequencies, which were remeasured for each test condition, as shown in Fig. 3. The solid lines in Fig. 3 represent the average of the measured frequencies. Wings 1A, 1B, and 1C were tested both at subsonic and supersonic conditions up to a Mach number of 3.0. Wings 2A, 2B, 2C were tested at supersonic conditions up to a Mach number of 3.0.

Vibration Modes

The vibration modes used in this study were calculated using finite element models. Figure 4 shows the model for Wing 1A, used here as an example of the finite-element model. This model is made up of fifty-five quadrilateral combined membrane and bending elements, eleven triangular combined membrane and bending elements, and twelve evenly spaced beam elements at the root. The stiffness of these beam elements at the root was varied in order to tune the frequencies to match the average of the measured frequencies. The beam elements attempt to model the clamping of the wind tunnel model. Sixteen vibration modes were calculated, the first seven of which were used for flutter calculations. The mode shapes for the first four vibration modes are shown in Fig. 5. In the experimental results the flutter frequency is nearly the second modal frequency. This mode is a torsional mode with the node line being orthogonal to the root at about 70 percent from the root leading edge and extending out the span.

Initially the experimentally measured modes were used in the flutter study. However these mode shapes were found to be nonorthogonal when the off diagonal generalized masses were calculated. The probable cause is the relatively few points which define the mode shapes and measurement accuracy. When the measured modes were used, the third or fourth modes were often found to cause "hump" modes which occurred at lower flutter speeds than the principle second mode crossing. Experimental results show that the flutter frequency is always close to the second natural vibration frequency.

Description of Flutter Analyses

The structural equations of motion were solved using the generalized aerodynamic forces from four different programs including: (1) "A Steady and Oscillatory Kernel Function Method for Interfering Surfaces in Subsonic, Transonic and Supersonic Flow" by Atlee Cunningham hereafter referred to as ACUNN,[2] (2) FAST,[4] (3) second order piston theory,[6] and (4) CAP-TSD[5]. Each of these programs is capable of calculating the aerodynamics for subsonic flows while ACUNN and CAP-TSD can calculate supersonic flows as well. Brief descriptions of each of the three codes (ACUNN, FAST and CAP-TSD) follow.

ACUNN is based on linear lifting surface theory and relates the pressure distribution on an oscillating wing to the downwash at specified control points. A structural surface spline in the code interpolates the mode shapes at the control points. The generalized forces are used by the STABCAR[3] program to perform the flutter calculations. STABCAR is a program which determines the characteristic roots of flexible aircraft by using a modal formulation integrated with the unsteady aerodynamic forces.

FAST, which stands for Flutter Analysis System, consists of a group of programs used to perform flutter calculations. A subsonic kernel function is used in calculating the generalized

forces. The mode shapes and flutter calculations are based on a V-g type of analysis. All of the calculations made with FAST use a 10x10 collocation grid.

CAP-TSD is an acronym for Computational Aeroelasticity Program - Transonic Small Disturbance. This code is based on the unsteady transonic small disturbance (TSD) equation and is capable of calculating unsteady flows about complete aircraft. The TSD equation is solved using an approximate factorization algorithm. CAP-TSD requires no special grid generating program since it uses a cartesian grid. This makes the modeling of complex geometries much simpler.

Results and Discussion

The following results consist of comparisons of experimental and theoretical flutter characteristics at the flutter boundary, namely, flutter speed index versus Mach number, and flutter frequency ratio versus Mach number.

Results for Wing 1A

The Wing 1A flutter boundary, Fig. 6, is plotted as flutter speed index, which is proportional to the square root of dynamic pressure, versus Mach number. The boundary predicted by FAST shows very good agreement with experiment. The supersonic results calculated with ACUNN show fairly good agreement with experiment although at Mach 2.5 a "hump" mode was present which caused a lower flutter speed to be predicted as indicated by the flagged triangle. The hump mode in this case was caused by Mode 3 going unstable first. The unflagged triangle at Mach 2.5 indicated the speed at which Mode 2 becomes unstable. In all the other calculations Mode 2 goes unstable first. The agreement between piston theory and experiment is surprisingly good even for the lower supersonic Mach numbers where piston

theory would not normally be considered to be applicable.

Figure 7 shows the lowest flutter speed (flagged triangle) corresponds to a frequency ratio that is approximately twice the experimental value. This rapid change in flutter frequency is characteristic of a "hump" mode. Comparisons between calculated results and experiment for the remaining points indicate good agreement in flutter frequencies.

Results for Wing 1B

The flutter boundary for Wing 1B, Fig. 8, predicted by FAST shows very good agreement with experiment. The supersonic results using ACUNN predict the general trend of experiment but go from being conservative to nonconservative as Mach number increases. It is interesting to note that the experimental flutter boundary drops slightly at Mach 2 and then begins to increase again. This feature is also apparent for Wing 1C. The piston theory results are again fairly good even at the lower supersonic Mach numbers.

Results for Wing 1C

For Wing 1C, FAST predicts a flutter boundary that is nonconservative although it does predict the general trend of experiment as shown in Fig. 9. The boundary predicted by ACUNN is in good agreement with experiment for low supersonic cases but becomes nonconservative for higher Mach numbers. Piston theory also predicts a nonconservative flutter boundary for the higher Mach numbers in agreement with ACUNN. The experimental flutter boundary, as noted earlier, drops off at Mach 2 but this time to a greater extent. A possible cause of the drop in the flutter boundary is the presence of a shock created by the wedge shaped mounting system at the tunnel wall. Such a shock could alter the flow conditions that the model experiences and thus the flutter boundary.

Wing 2A Results

The results calculated with FAST show the flutter boundary trend predicted for Wing 2A at subsonic Mach numbers. These results are shown in Fig. 10. Unfortunately there is no experimental data available in the subsonic region. The supersonic calculations with ACUNN and piston theory both predict a flutter boundary that is very conservative. The reason for this is not fully understood though a possible cause is that the finite element model could not be tuned to match the experimental frequencies within a few percent. In fact, the second vibration frequency could only be tuned to within 15% of the experimentally measured values, possibly causing the mode shapes to be insufficiently representative for accurate flutter analysis.

Results for Wing 2B

Figure 11 shows the subsonic FAST results predict a trend which appears to be a reasonable extrapolation of the experimental trend in the supersonic region. Such thin wings may not have a significant transonic dip and such an extrapolation of the flutter boundary is reasonable. The supersonic results for both ACUNN and piston theory are in very good agreement with experiment.

Results for Wing 2C

The subsonic flutter boundary predicted with FAST for Wing 2C again matches the trend of the supersonic data fairly well as seen in Fig. 12. Supersonic calculations with ACUNN and piston theory predict a flutter boundary that is nonconservative although they do predict the trend of the flutter boundary quite well.

CAP-TSD Calculations

When using CAP-TSD for the 70 degree delta wing it was necessary to clip off (aerodynamically) 10% of the wing tip. The purpose for clipping the tip was to generate a grid, since lines must be extended from the leading and trailing edges to the outer boundary in a smooth fashion as shown in Fig. 14. The mode shapes used were from the full span model. The effect of clipping the wing for subsonic speeds was studied using FAST and it was found that clipping the wing up to 10% did not effect the calculated flutter boundary (Fig. 13). Since grid lines extending from the root to the outer boundary are of constant percent chord problems arise for highly swept wings - especially for ones with a low taper ratio. Because of high sweep, the grid becomes highly skewed and can cause poorer convergence. The low taper ratio also causes the grid lines to be tightly packed at the tip which gives rise to large changes in grid metrics. This can also give rise to poorer convergence. Thus care must be taken in gridding highly swept wings.

The results shown in Figure 15 were calculated with CAP-TSD. Wing 1A was modeled as a flate plate. The flutter boundary was calculated for several Mach numbers and very good agreement with experiment was obtained. Comparing CAP-TSD with the subsonic results from FAST (Fig. 6) shows nearly identical agreement as should be the case. The good agreement indicates that CAP-TSD can be applied to a highly swept wing and builds confidence in the code prior to treating more complex configurations such as adding in thickness, fuselage, etc.

Concluding Remarks

The flutter characteristics of six delta wings were studied with leading-edge sweep angles ranging from 54° to 80°. The aerodynamics used in solving the structural equations came from ACUNN, FAST, piston theory, and CAP-TSD. Comparisons among the different aerodynamic

methods show that all the methods give fairly good results although the results shift from being conservative to nonconservative.

References

[1]Hanson, P. W.; and Levey, G. M.: "Experimental and Calculated Results of a Flutter Investigation of Some Very Low Aspect-Ratio Flate-Plate Surfaces at Mach Numbers from 0.62 to 3.00," NASA TN D-2038, October 1963.

[2]Cunningham, A. M., Jr.: "A Steady and Oscillatory Kernel Function Method for Interfering Surfaces in Subsonic, Transonic and Supersonic Flows," NASA CR-144895, 1976.

[3]Adams, W. M., Jr.; Tiffany, S. H.; Newsom, J. R.; and Peele, E. L.: "STABCAR - A Program for Finding Characteristic Roots of Systems Having Transcendental Stability Matrices," NASA TP-2165, 1984.

[4]Desmarais, R. N.; and Bennett, R. M.: "Users Guide for a Modular Flutter Analysis System," NASA TM 78720, May 1978.

[5]Batina, John T.; Seidel, David A.; Bland, Samuel R.; Bennett, Robert M.: "Unsteady Transonic Flow Calculations for Realistic Aircraft Configurations," NASA TM 89120, 1987.

[6]Ashley, Holt and Zartarian, Garabed: "Piston Theory - A New Aerodynamic Tool for the Aeroelastician," Journal of Aeronautical Sciences, Volume 23, No. 12, Dec. 1956, pp. 1109-1118.

Model 1A

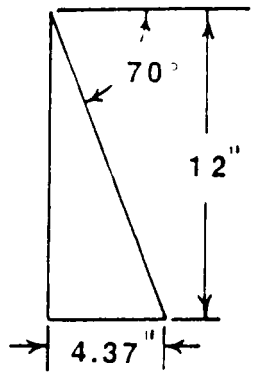

A = 0.728
W = 0.0794 lb
t = 0.032 in
δ = 3/32 in

Model 1B

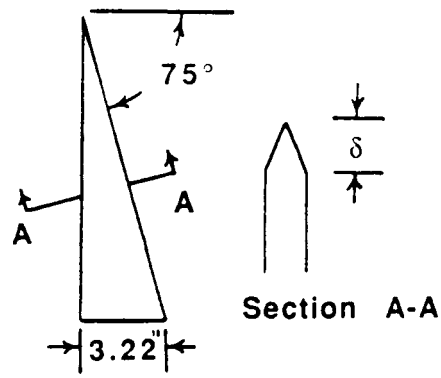

A = 0.536
W = 0.0573 lb
t = 0.032 in
δ = 3/32 in

Model 1C

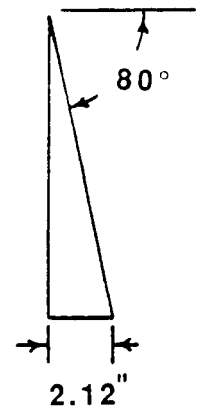

A = 0.353
W = 0.0322 lb
t = 0.026 in
δ = 1/16 in

Model 2A

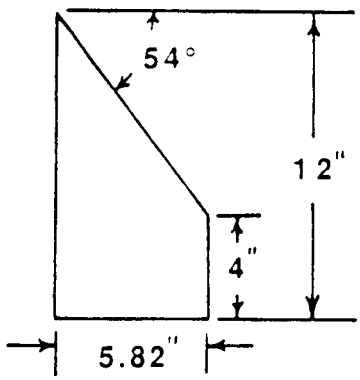

A = 0.728
W = 0.143 lb
t = 0.032 in
δ = 3/32 in

Model 2B

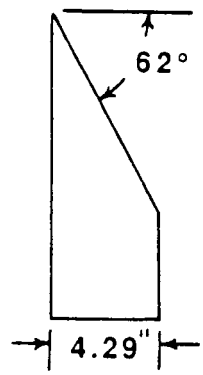

A = 0.536
W = 0.106 lb
t = 0.032 in
δ = 3/32 in

Model 2C

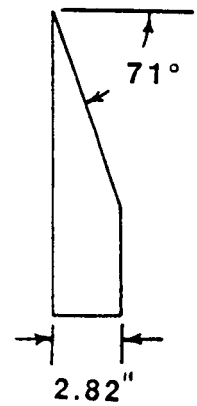

A = 0.353
W = 0.0694 lb
t = 0.032 in
δ = 1/16 in

Fig. 1 Wind tunnel models from TN D-2038

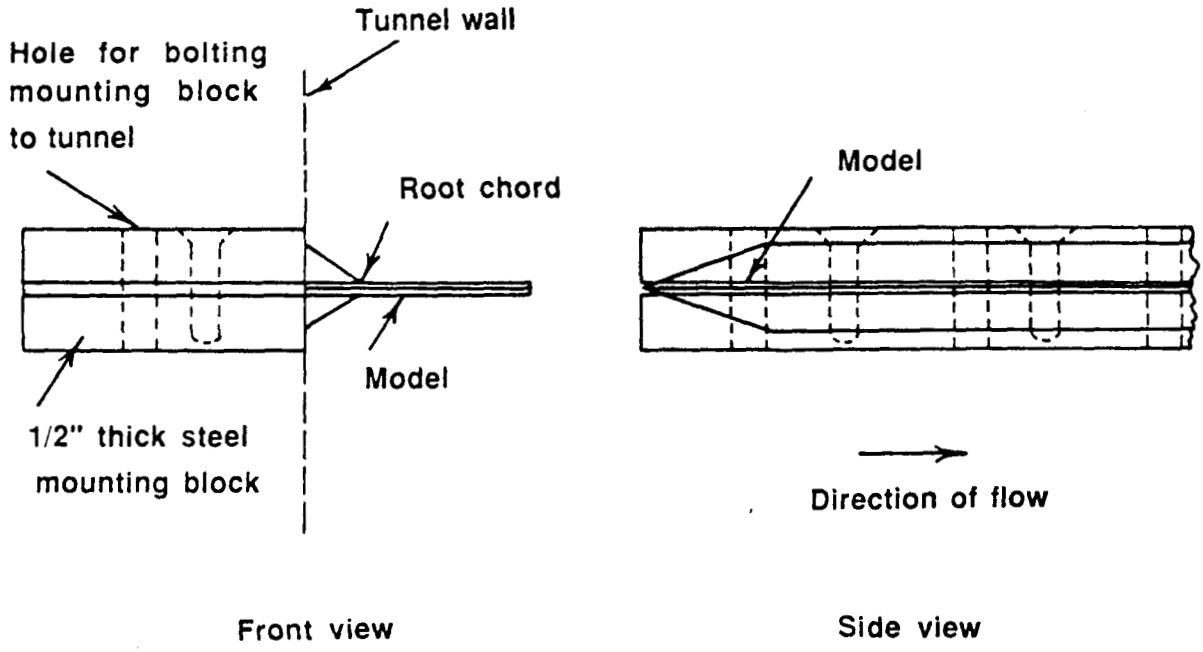

Fig. 2 Method used for mounting models in tunnel

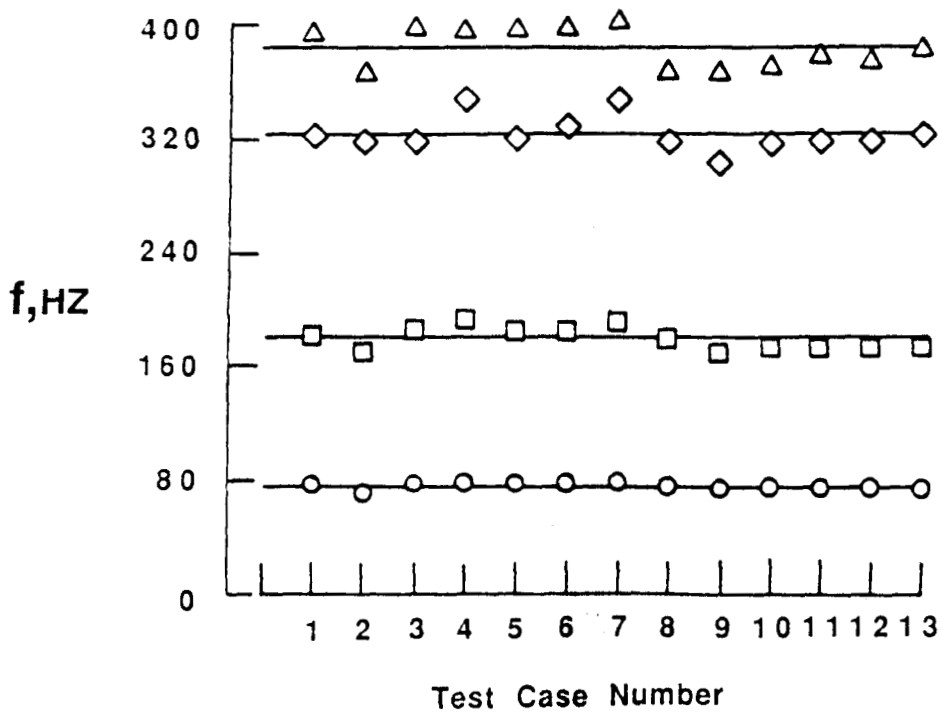

Fig. 3 Modal frequency variation for 70° delta wing

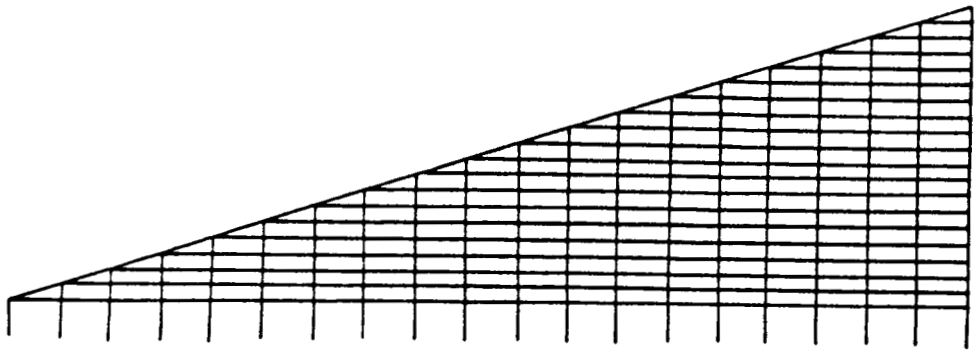

Fig. 4 Finite elment model for 70° delta wing

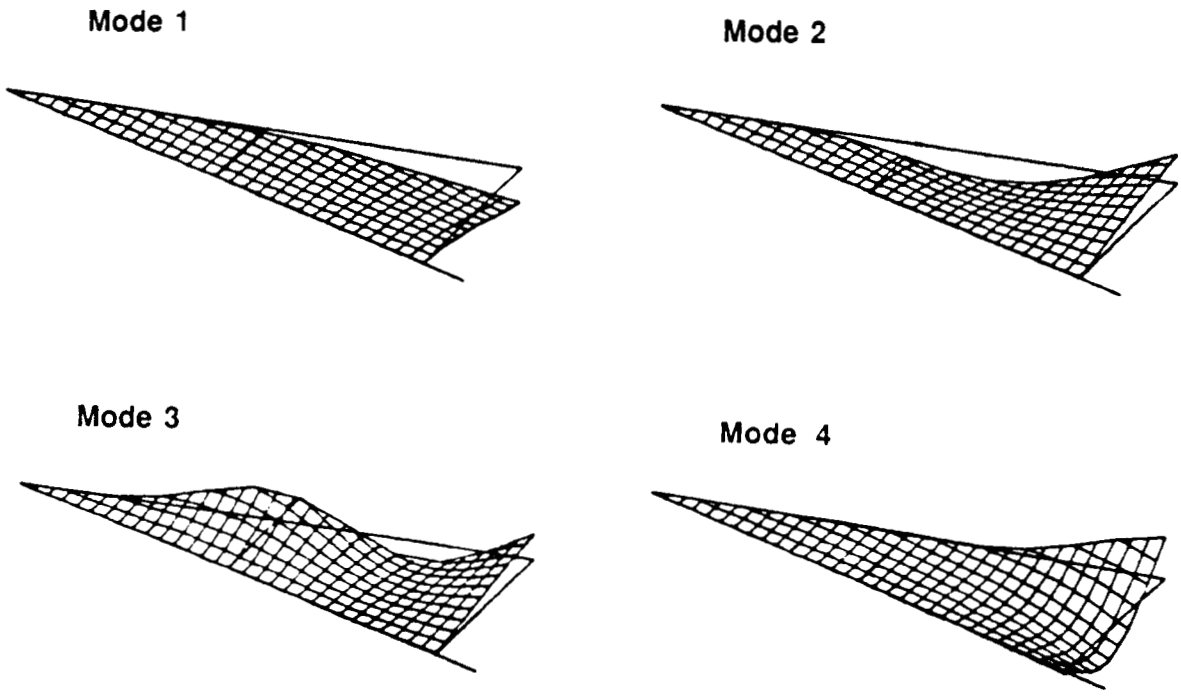

Fig. 5 Mode shapes for 70° delta wing

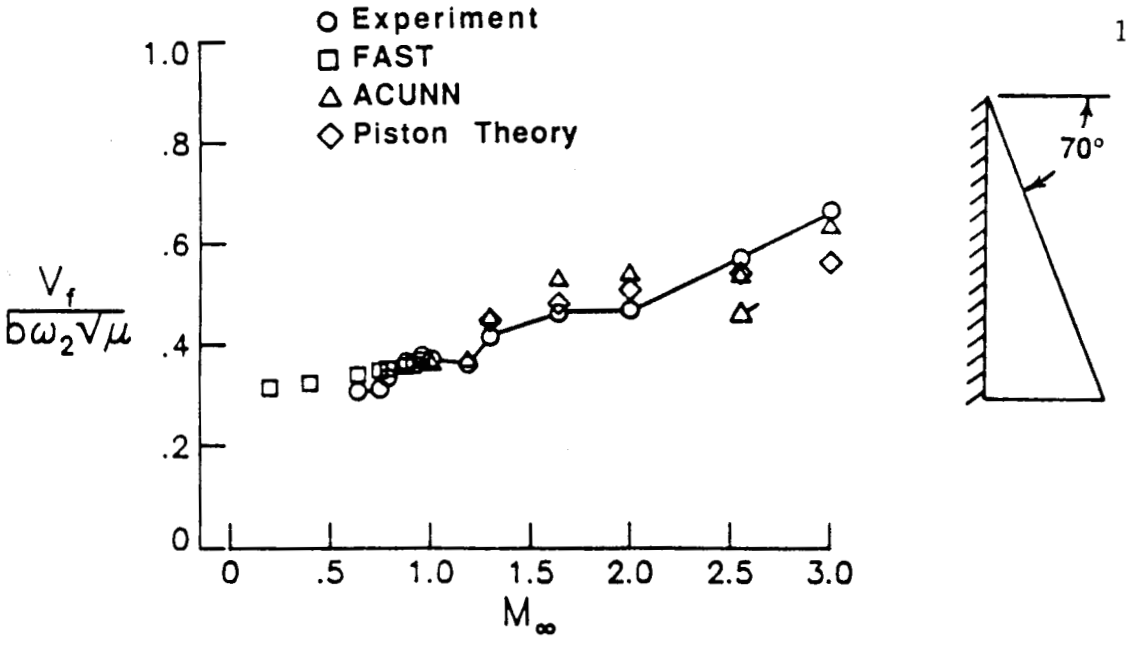

Fig. 6 Experimental and analytical flutter boundary for 70° delta wing 1A using linear and piston theory

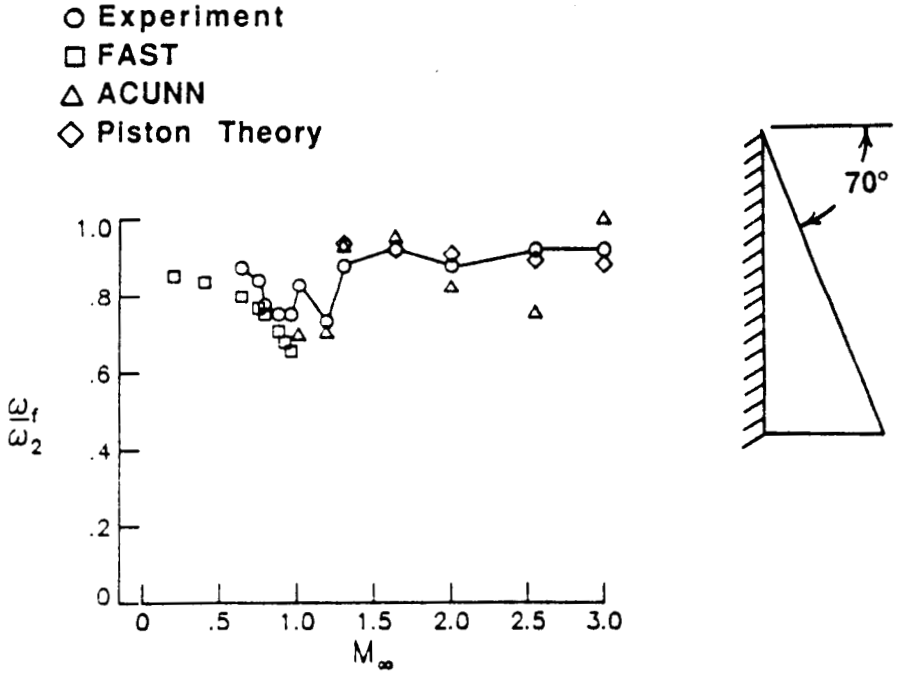

Fig. 7 Experimental and analytical flutter frequency ratios for 70° delta wing 1A using linear and piston theory

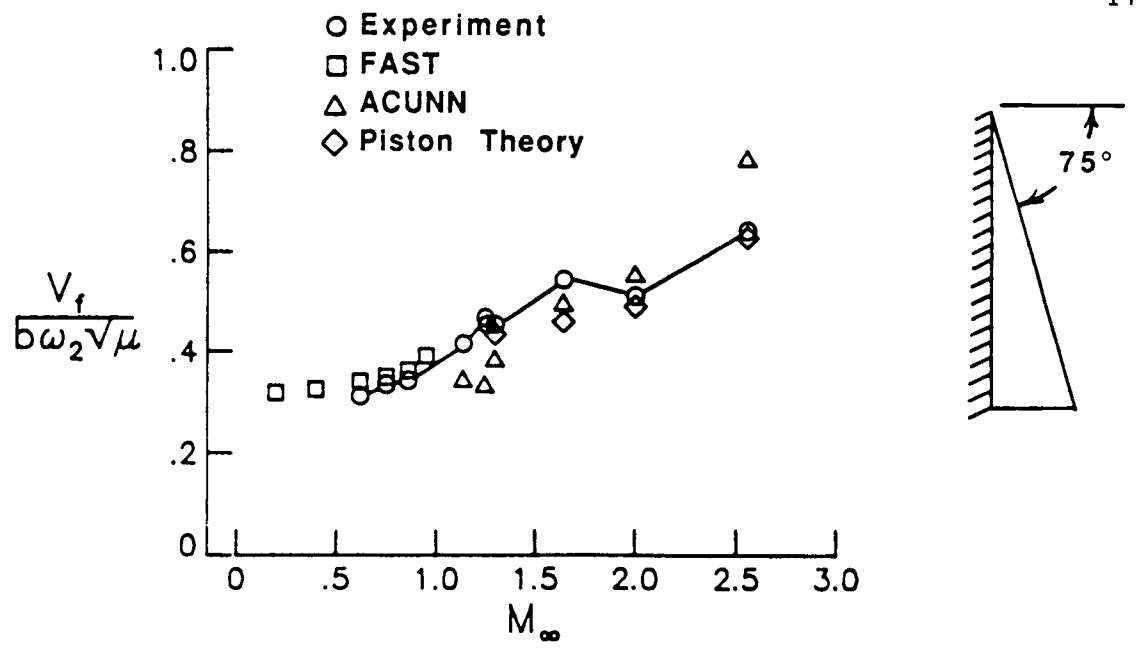

Fig. 8 Experimental and analytical flutter boundary for 75° delta wing 1B using linear and piston theory

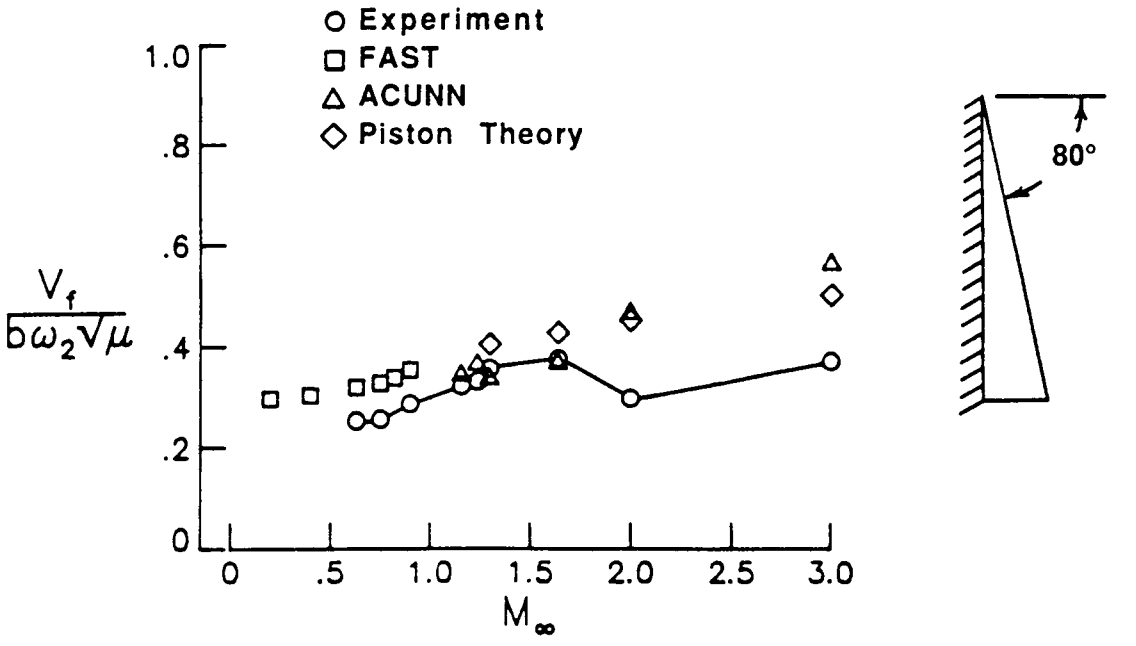

Fig. 9 Experimental and analytical flutter boundary for 80° delta wing 1C using linear and piston theory

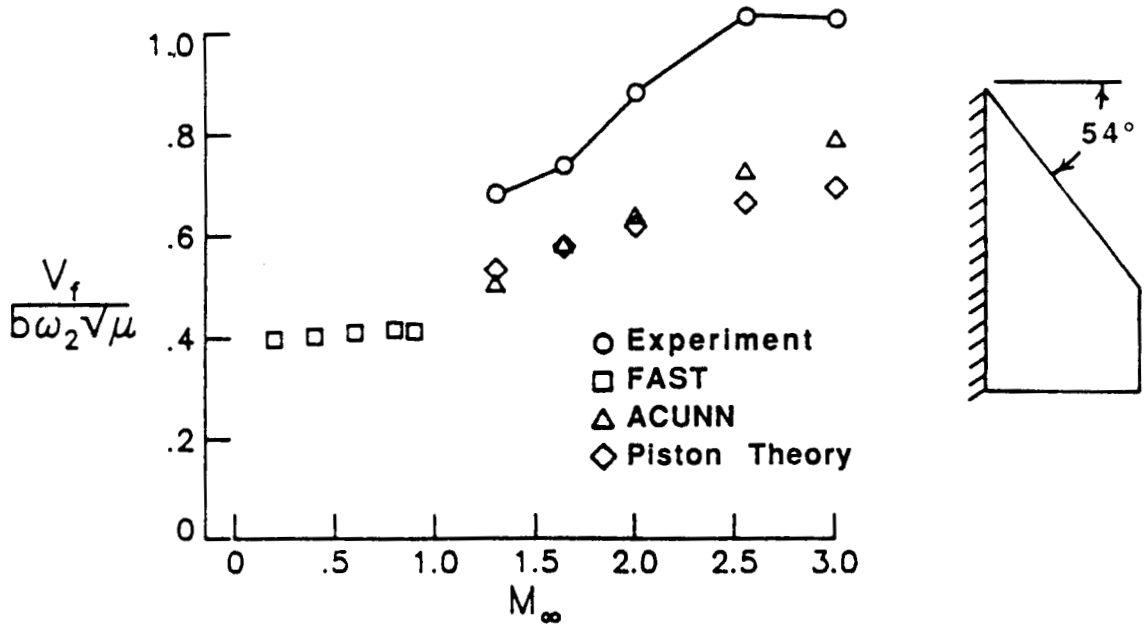

Fig. 10 Experimental and analytical flutter boundary for 54° clipped delta wing 2A using linear and piston theory

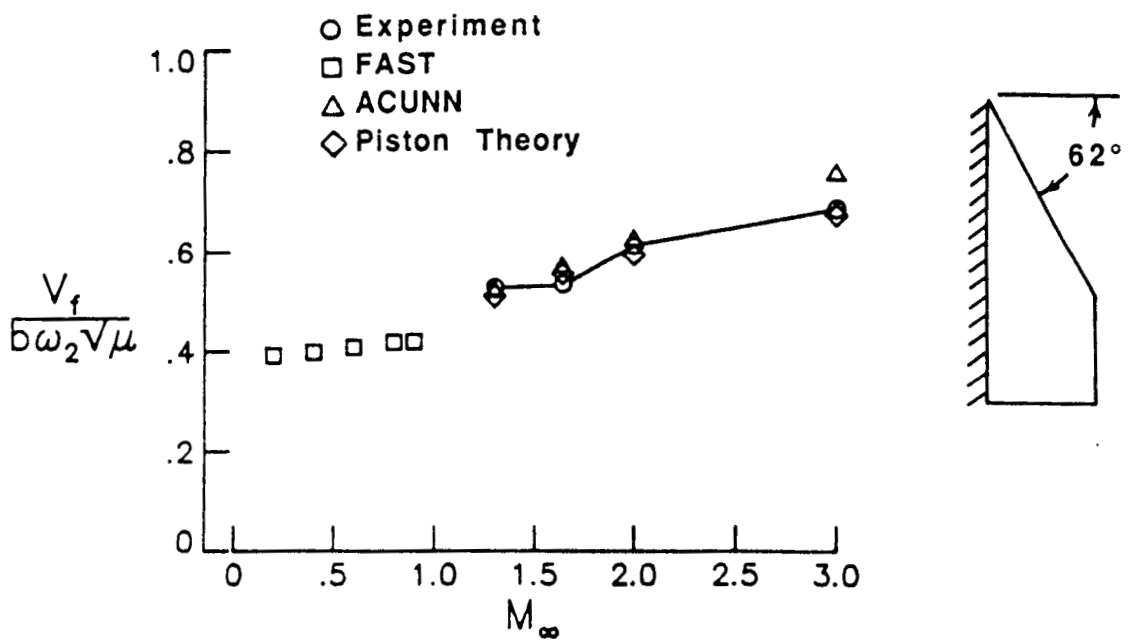

Fig. 11 Experimental and analytical flutter boundary for 62° clipped delta wing 2B using linear and piston theory

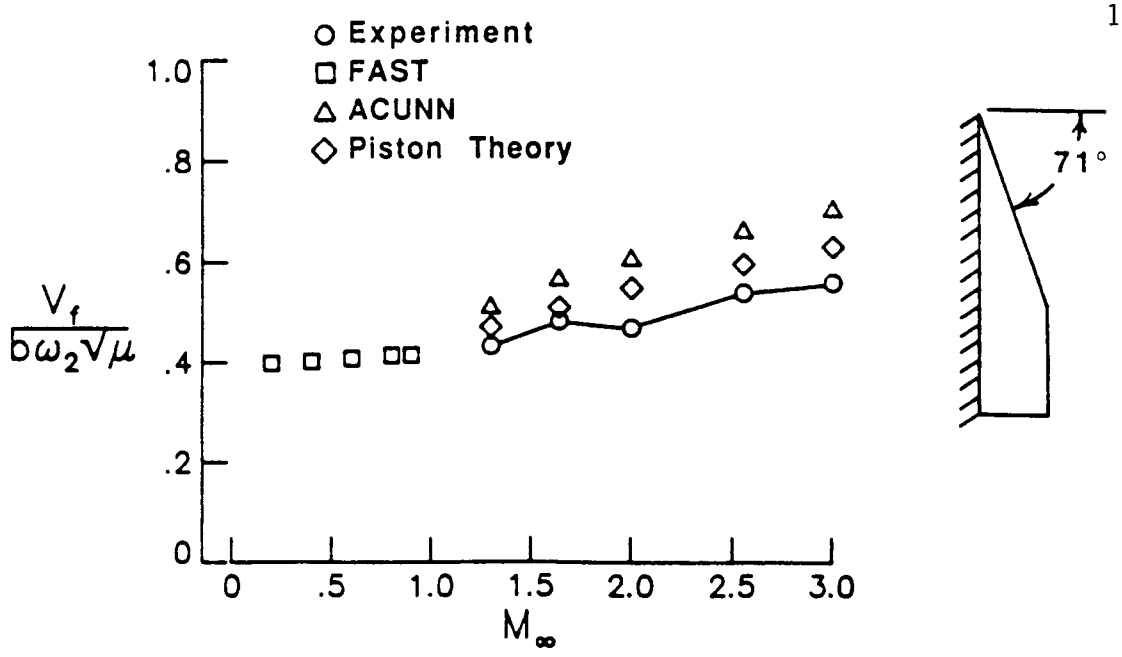

Fig. 12 Experimental and analytical flutter boundary for 71° clipped delta wing 2C using linear and piston theory

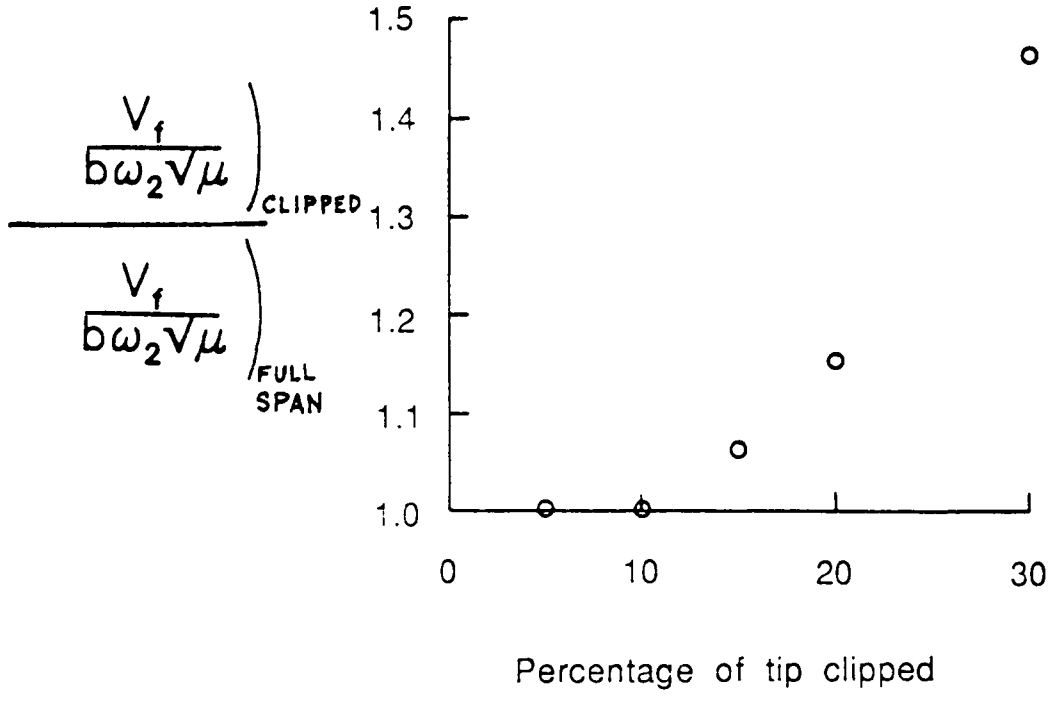

Fig. 13 Effects of aerodynamically clipping the tip of wing 1A on flutter speed index

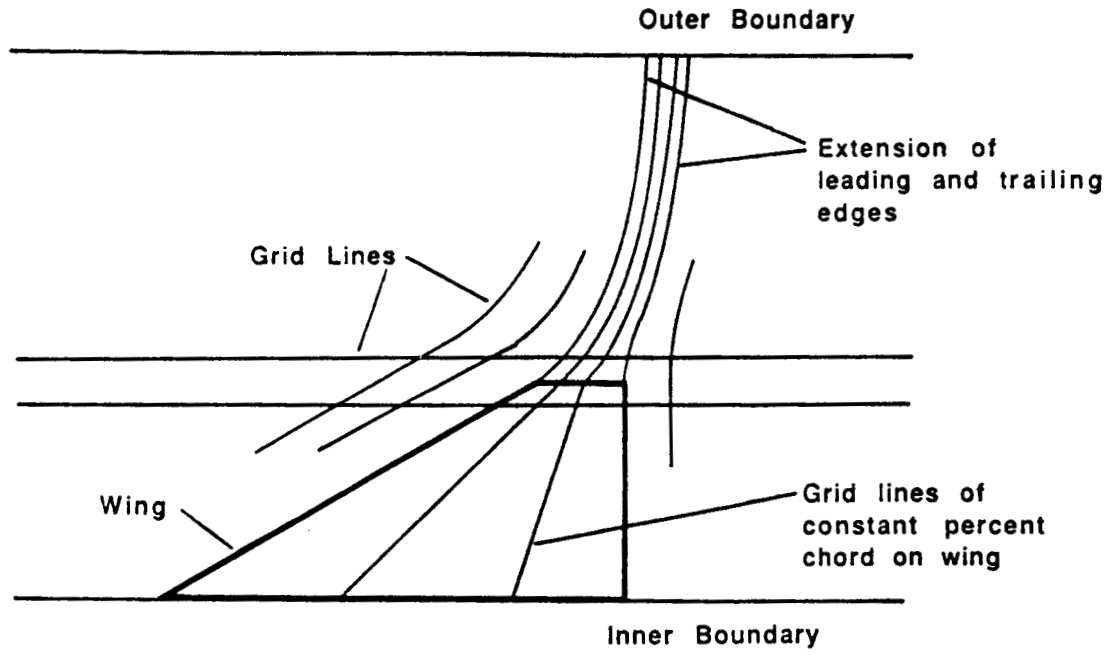

Fig. 14 CAP-TSD computational grid for 70° delta wing

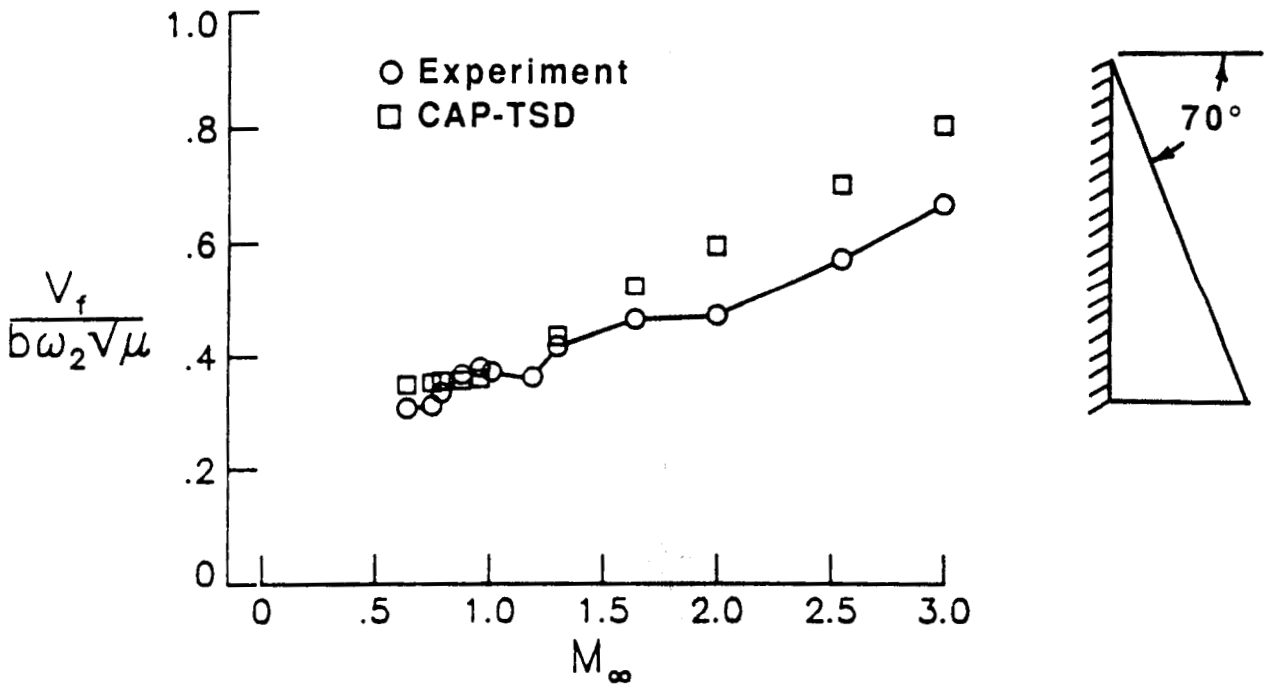

Fig. 15 Experimental and analytical flutter boundary for 70° delta wing using CAP-TSD

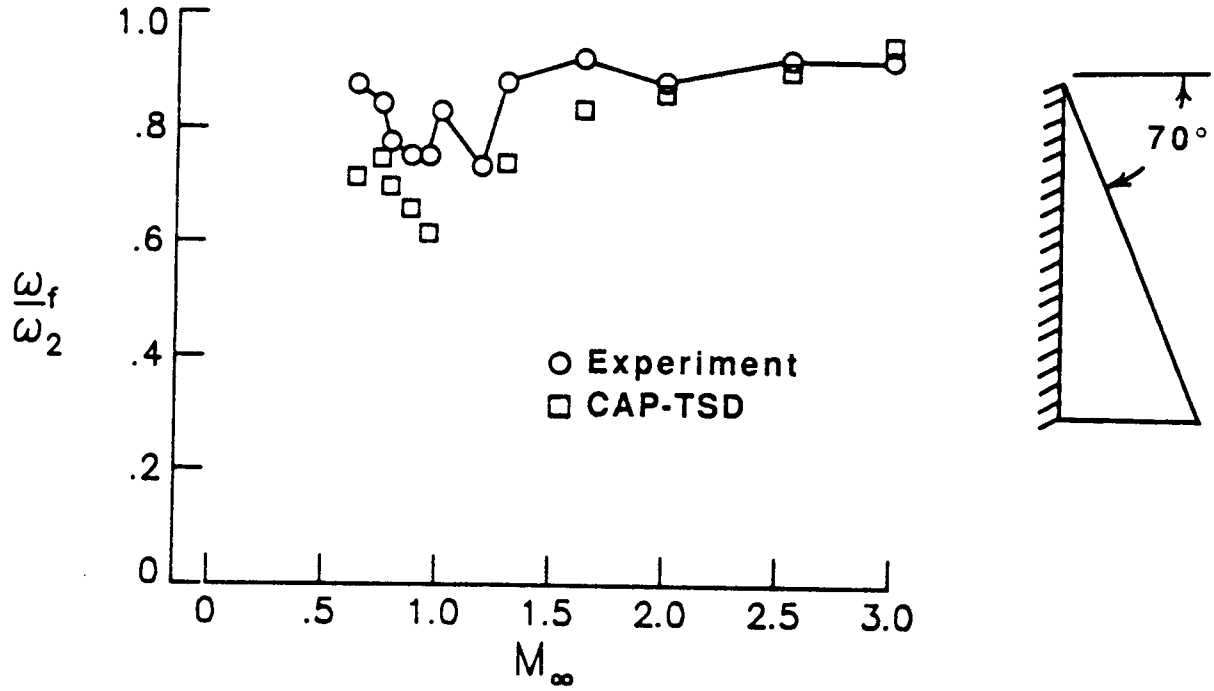

Fig. 16 Experimental and analytical flutter frequency ratios for 70° delta wing using CAP-TSD

NASA National Aeronautics and Space Administration

Report Documentation Page

1. Report No.	2. Government Accession No.	3. Recipient's Catalog No.
NASA TM-101530		

4. Title and Subtitle
Flutter Analysis of Highly Swept Delta Wings by Conventional Methods

5. Report Date
November 1988

6. Performing Organization Code

7. Author(s)
M. D. Gibbons
D. L. Soistmann
R. M. Bennett

8. Performing Organization Report No.

10. Work Unit No.
505-63-21-01

9. Performing Organization Name and Address
NASA Langley Research Center
Hampton, Virginia 23665-5225

11. Contract or Grant No.

13. Type of Report and Period Covered
Technical Memorandum

12. Sponsoring Agency Name and Address
National Aeronautics and Space Administration
Washington, DC 20546-0001

14. Sponsoring Agency Code

15. Supplementary Notes
M. D. Gibbons and D. L. Soistmann: PRC Systems Services, Hampton, Virginia.
R. M. Bennett: Langley Research Center, Hampton, Virginia.

16. Abstract
The flutter boundaries of six thin highly-swept delta-planform wings have been calculated. Comparisons are made between experimental data and results using several aerodynamic methods. The aerodynamic methods used include a subsonic and supersonic kernel function, second order piston theory, and a transonic small disturbance code. The dynamic equations of motion are solved using analytically calculated mode shapes and frequencies.

17. Key Words (Suggested by Author(s))
Flutter
Delta Wings
Aeroelasticity
FAST, Piston theory, CAP-TSD

18. Distribution Statement
Unclassified - Unlimited
Subject Category - 02

19. Security Classif. (of this report)	20. Security Classif. (of this page)	21. No. of pages	22. Price
Unclassified	Unclassified	19	A02